INSTITUTE OF PHYSICS PUBLISHING JOURNAL OF PHYSICS D: APPLIED PHYSICS

J. Phys. D: Appl. Phys. **38** (2005) 950–954 doi:10.1088/0022-3727/38/6/027

Particle-in-cell simulation of gas breakdown in microgaps

M Radmilović-Radjenović, J K Lee, F Iza and G Y Park

Electronics and Electrical Engineering Department, Pohang University of Science and Technology, Pohang, 790-784, Korea

Received 30 November 2004, in final form 6 January 2005
Published 3 March 2005
Online at stacks.iop.org/JPhysD/38/950

Abstract

Gas breakdown in large scale systems has been widely studied and is reasonably well understood. Deviations from the well-known Paschen law, however, have been reported in microgaps. One possible mechanism responsible for these deviations is the increase of the secondary electron emission yield due to the quantum tunnelling of electrons from the metal electrodes to the gas phase. The high electric fields obtained in small gaps combined with the lowering of the potential barrier seen by the electrons in the cathode as an ion approaches lead to the onset of ion-enhanced field emissions. Particle-in-cell/Monte Carlo simulations including ion-enhanced field emission have been performed to evaluate the importance of these mechanisms in the discharge breakdown. Deviations from the Paschen curve in gaps smaller than 5 μm can be explained based on this mechanism.

1. Introduction

Recently, much attention has been paid to mesoscale and nanoscale systems in various fields of science including physics, chemistry, material science, electronics and metrology [1]. Many interesting phenomena such as quantum effects have been observed in these small scale systems [2–5]. Studies, however, have been mostly focused on mesoscale/nanoscale domains in solid state materials. Nevertheless, quantum effects and deviations from the behaviour of large scale systems as scale is reduced can be expected in other fields of science including plasmas [5].

In this paper, gas breakdown in micrometre and submicrometre size gaps is studied by means of computer simulations. In recent years, computer modelling and simulation has emerged as an effective tool that complements laboratory experiments and analytic models. Plasma simulation codes [6, 7] have acquired a high level of sophistication and are routinely used in the design of plasma reactors for the semiconductor industry. Furthermore, the difficulty in achieving well-defined experimental conditions and the limited diagnostic techniques available for small scale discharges, favour the investigation of meso/nano scale systems with simulation tools. Particle-in-cell (PIC) and particle-in-cell/Monte Carlo (PIC-MC) simulations have been extensively used to study fundamental processes in capacitively coupled radio frequency discharges [8–10] and plasma display panels [11, 12]. To the author's knowledge, however, no attempt has been made so far to model gas breakdown in submicrometre scale gaps.

Understanding the mechanisms responsible for gas breakdown is of interest not only to the plasma community but also to the microelectronics industry. Integrated circuits, MEMS, magnetic recorders and flat panel displays, to name a few, all have features with dimensions in the micrometre and submicrometre range. The continued downscaling of these devices, therefore, requires an understanding of the mechanisms responsible for the gas breakdown in order to prevent undesired sparks that can lead to device malfunction or failure during manufacturing, handling and operation [13, 14].

Deviations from Paschen's theory in microgaps were first reported in the 1950s by Germer and Kisluik [15, 16] in a series of papers that studied submillimetre electrode spacings. Later, Torres and Dhariwal [17] provided an explanation for the deviation based on quantum tunnelling of electrons during a study of micromotors and microactuators. Lee *et al* [18] observed similar results while investigating electrode erosions caused by arc discharges. Slade and Taylor [19] compared the work done by Torres and Dhariwal [17] and Lee *et al* [18] and applied a linear-fit equation to the breakdown voltage versus the gap data. They also introduced the effect of cathode microprojections into the Fowler–Nordheim equation [4] to quantify the role of field emissions in the breakdown process.

The simulation results presented in this paper show that electrical breakdown across micrometre and submicrometre size gaps may occur at voltages far below the minimum predicted by the Paschen curve. This breakdown voltage reduction is observed for gap sizes smaller than 5 μm and is a consequence of the onset of ion-enhanced field emission [2–5].

2. Gas breakdown theory

2.1. DC breakdown

In large scale systems, the experimentally observed Paschen law has been successfully explained by the Townsend theory [20]. Paschen curves dictate the breakdown voltage for a particular gas as a function of the *pd* (pressure times electrode distance) product. This breakdown voltage curve represents a balance between the number of electrons lost by diffusion and drift in the inter-electrode gap and the number of secondary electrons generated at the cathode [20]. Over a large range of pressures and electrode separations, the probability of ionization per electron–neutral collision in the gas and the probability of the production of secondary electrons by ion bombardment of the cathode are proportional to E/N [21] and lead to the well-established *pd* similarity law.

Paschen curves are roughly U-shaped and present an optimum *pd* value for which the breakdown voltage is minimum. At *pd* values lower than the optimum, not enough collisions take place before the electrons are lost to the anode and an abrupt increase in the breakdown voltage is observed. In microgaps, however, gas breakdown at voltages lower than the minimum predicted by the Paschen curve and at *pd* values for which the Paschen curve suggests extremely large breakdown voltages has been observed. It was suggested that the high fields obtained in small gaps may enhance the secondary emission coefficient and that such enhancement would lead to a lowering of the breakdown voltage and a departure from the Paschen curve [22].

Current models of secondary electron emissions in low fields require ions to be neutralized as a first step in the emission process. Therefore, single-charged ions are capable of extracting a maximum of one electron. The mechanism, however, is quite different in the presence of high electric fields [23, 24]. When the electric field near the cathode is sufficiently large, electron tunnelling from the metal to the gas phase needs to be taken into account. Furthermore, as an ion approaches the cathode, it lowers the potential barrier seen by the electrons in the metal resulting in an ion-enhanced electron field emission [22]. An explicit expression for the electron yield per ion (γ) that incorporates this ion-enhanced field emission is given by [22]:

$$\gamma = K\mathrm{e}^{-B/E}, \tag{1}$$

where K and B are material and gas dependent constants and E is the electric field near the cathode. This theoretical relation is a direct consequence of the theory of field emission breakdown [4, 5, 22].

When the electric field in the cathode region becomes larger than the threshold value given by B, the electron yield per ion increases rapidly. Since field emission is mainly governed by the electric field E rather than the reduced electric field E/N, deviations from the Paschen curve are expected when the secondary emission process is governed by ion-enhanced field emissions rather than ion impact.

2.2. Microwave breakdown

As long as the electrons and ions have sufficient time to transit the electrode gap within an ac cycle, the gas breakdown mechanism in low frequency alternating electric fields is essentially the same as for dc fields, i.e. it is controlled by secondary electron emission due to ion impact. At sufficiently high frequencies, however, ions are not capable of responding to the ac field and electrons are 'trapped' in an oscillatory motion within the inter-electrode gap. When this occurs, the electron loss is dominated by diffusion and a significant reduction of the breakdown voltage is observed as compared to the dc case [25]. As in the case of dc discharges, however, departures from the large scale similarity laws are expected with the onset of field emissions in small gaps.

3. Simulation codes: the PIC/Monte Carlo model

The simulation codes used in this work are based on XPDP1 and XPDC1 [6, 7]. Modifications to these codes include the introduction of the ion-enhanced field emission mechanism described in section 2 as well as secondary electron emissions due to electron impact [26] and the energy and angle dependent ion bombardment [27]. The codes are one-dimensional bounded electrostatic PIC codes [6, 7, 9, 28–30] with Monte Carlo treatment of collisional processes. DC simulations were performed using the modified XPDP1 code and microwave simulations using the modified XPDC1. PIC modelling techniques have been described in detail in many publications (see for example, [6, 7, 9, 28–30]) so only a brief description of the code will be given here.

In PIC simulations, the so-called 'super-particles' move in the discharge space through an artificial grid on a time step basis. Only charged particles are simulated. At the beginning of the simulation, super-particles are distributed in the simulation domain and a self-consistent potential distribution is determined based on the super-particles positions and the externally applied voltage. This is done by weighting the particles to the grid points and solving Poisson's equation. The simulation proceeds by calculating the electric field and weighting it to the particle positions. The force exerted by the electric field is then computed and particle velocities and positions are updated. A Monte Carlo algorithm is used to account for the collisional processes. The null-collision method introduced by Vahedi and Surendra [7] is used.

The Monte Carlo collision (MCC) model describes the collision processes using statistical methods and cross sections for each reaction. As we use 1 million super-particles for each target species, computing the collision probability for all the particles at each time step can be computationally very expensive. Instead, the more efficient method of null collision probability is used in the codes. For each type of projectile we can determine a total collision probability independent of particle energy and position as:

$$P_{\mathrm{t}} = 1 - \exp(-\nu_{\max}\,\mathrm{d}t),$$

where dt is the time interval and $\nu_{\max}$ the maximum collision frequency is given by:

$$\nu_{\max} = N_{\mathrm{g}} \max_{\varepsilon}(\sigma_{\mathrm{t}}(\varepsilon)v(\varepsilon)).$$

In the above equation, N_{g} is the spatially uniform neutral density, $v(\varepsilon)$ is the incident speed of a particle with energy ε and the total cross section $\sigma_{\mathrm{t}}(\varepsilon)$ represents the sum over all processes j:

$$\sigma_{\mathrm{t}}(\varepsilon) = \sum_{j} \sigma_j(\varepsilon).$$

The number of projectile particles dn taking part in collisions at each time step is given by the total collision probability:

$$\mathrm{d}n = P_{\mathrm{t}} n$$

and these particles are chosen at random from the particle list. The type of collision for each particle is determined by a random number. Further details concerning differential cross sections for ionization and elastic scattering of electrons, fractional energy loss corresponding to the scattering events, transformations from the centre-of-mass to the laboratory frame and so on are given in [7, 30].

XPDP1 was used to study dc breakdown at pressures between 1 and 6 atm whereas XPDC1 was used to study microwave breakdown at pressures ranging from 1 to 50 atm. Depending on the gas pressure, the time step dt was varied between 10^{-18} and 10^{-16} s. The gap size was varied from 0.1 to 10 μm. One million computer particles were used initially in each simulation.

In order to determine the breakdown voltage, we use the fact that the breakdown is not an instantaneous phenomenon. Break-down occurs over a finite period of time which is determined by the balance between the creation of charged species by ionization and their loss via collisional processes and diffusion to the walls. For each gas pressure, the time evolution of the electron density was observed and depending on its increasing or decreasing nature, the interval in which the breakdown voltage lies could be found through trial and error. Thus, for each gas pressure several simulations were performed.

All simulations were carried out with argon as a filling gas. Neutral atoms were assumed to be uniformly distributed throughout the simulation domain with a Maxwellian velocity distribution at room temperature (0.026 eV). The collision processes considered in the simulation include momentum-transfer, excitation and ionization collisions for electrons and momentum-transfer and charge exchange for ions. Calculations were performed using well established cross sections for argon [30, 31].

The energy and angle dependency of the yield per ion was taken from [27], while values for the K and B constants in the expression for the ion-enhanced field emission (equation (1)) were obtained from [5].

4. Simulation results and discussions

4.1. DC discharges

Figure 1 shows the simulated Paschen curves for argon in 10, 5 and 1 μm gaps. In the case of 10 and 5 μm gaps, the simulation

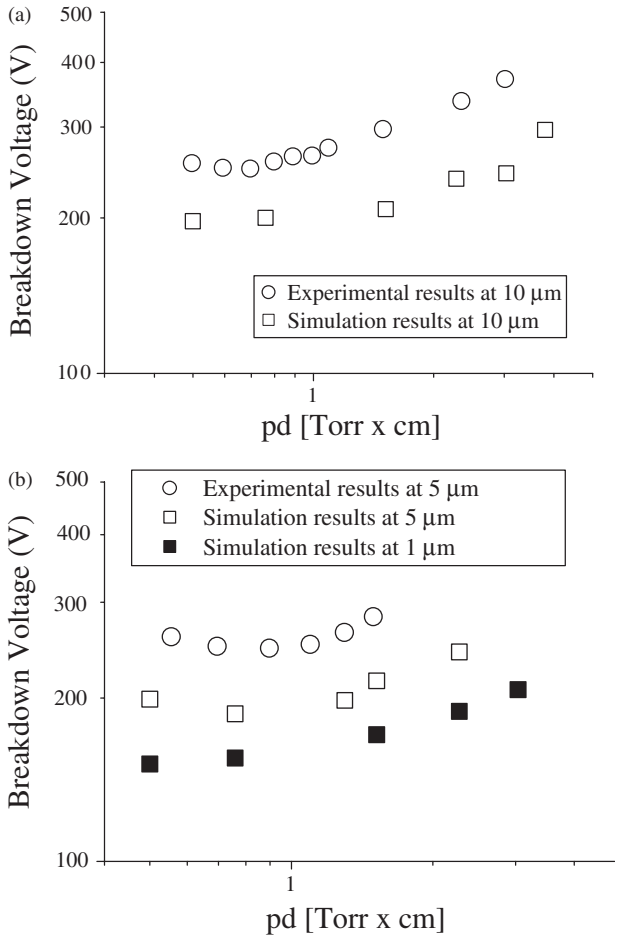

Figure 1. Breakdown voltage as a function of the pressure–gap spacing product for argon in (*a*) 10 μm and (*b*) 5 μm (open symbols) and 1 μm (solid symbols) gap. In the case of 10 and 5 μm gaps, the simulation results are compared with the experimental data obtained by Ito *et al* [32].

results are compared with the experimental data obtained by Ito and coworkers [32]. No experimental data are available for the 1 μm case. Similar trends are observed for the simulation and experimental results. The minimum breakdown voltage occurs at 6 Torr cm for the 10 μm gap and moves slightly to a higher pd value of 8 Torr cm in the 5 μm case. The lower breakdown voltage obtained in the simulations as compared to the experimental data is attributed to differences between the simulation and experimental conditions. Although the same gap size is used in both cases, the temperature and electrode materials used in the experiments are unknown [32]. Differences in temperature and secondary emission coefficients are believed to cause the breakdown voltage difference observed in figure 1 between the simulations and experimental results.

In gaps larger than 5 μm, field emissions can be neglected. As gap size is reduced, however, the electric field increases, ion-enhanced field emissions become important and a lowering of the breakdown voltage is observed (figure 1(*b*)). When this occurs, a departure from the Paschen curve is observed. Figure 2(*a*) shows the breakdown voltage as a function of gap size for argon at 1 atm. Two curves are plotted. The first one (circles) is obtained by using a conventional expression for the

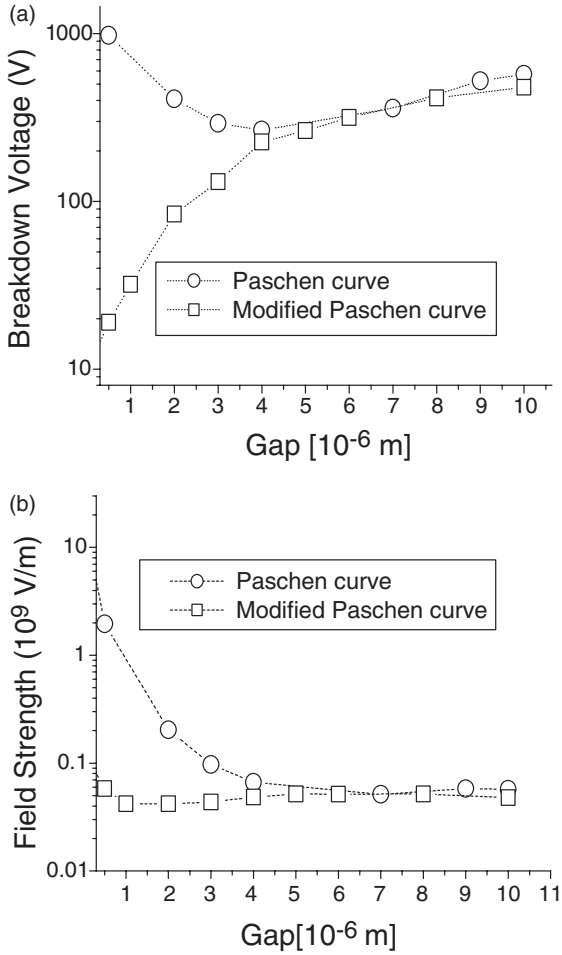

Figure 2. (*a*) Breakdown voltage and (*b*) electric field strength as a function of the gap size for argon at 1 atm. Results obtained by using energy and angular dependence of the yield per ion [27] (○) are compared with the results obtained when field-emissions are taken into account (□).

yield per ion [27] that does not account for ion-enhanced field emissions. The second one (squares) includes field emissions [22]. For relatively large gaps, a good agreement is found between both simulations. For gaps smaller than $\sim 5\,\mu$m, however, significant differences can be observed. In these small gaps, breakdown is no longer controlled by the processes within the gas. At 1 atm, the electron mean path is of the order of a few micrometres so at small inter-electrode spacings breakdown is initiated by the secondary emission processes instead of a gas avalanche process. A rapid fall of the breakdown voltage with decreasing gap size is associated with the presence of high electrical fields. The exponential dependency of the field emissions on the electric field strength pins the electric field during breakdown to the threshold for field emissions (figure 2(*b*)) and allows for a rapid reduction of the breakdown voltage as gap size is reduced (figure 2(*a*)). Similar experimental results have been reported by Torres and co-workers [17, 33].

4.2. Results for microwave discharges

Figure 3 shows the breakdown electric field strength in a 600 μm gap as a function of pressure for argon at

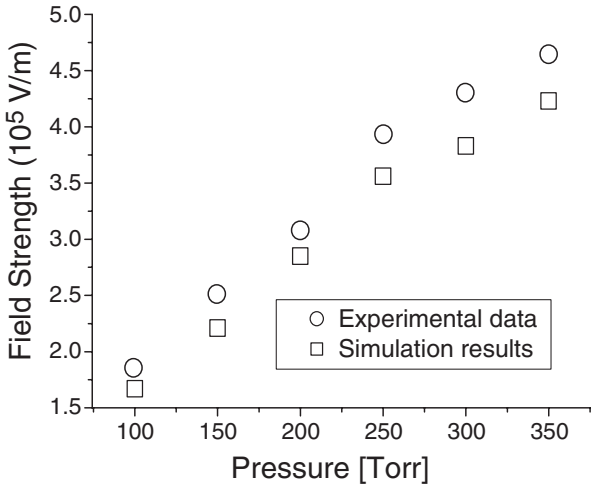

Figure 3. Electric field strength versus the pressure for an argon microwave discharge at 2.45 GHz. Experimental data [34] has been added for comparison.

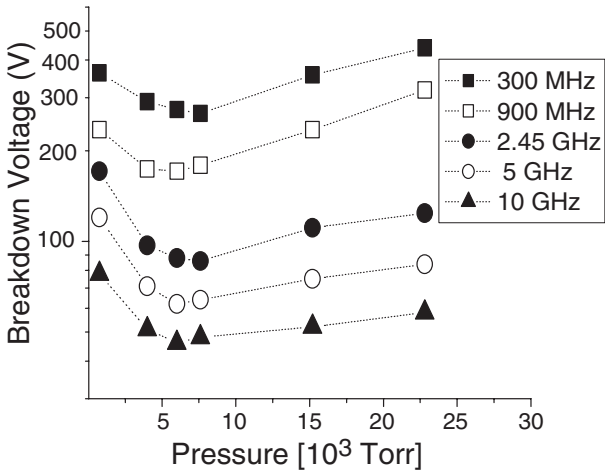

Figure 4. Dependence of the argon breakdown voltage on the pressure in a 1 μm gap at different frequencies.

2.45 GHz. Comparison with experimental data [34] shows good agreement. In order to explore the effect of ion-enhanced field emissions in high frequency discharges, simulations of a 1 μm gap were also performed. Frequency was varied from 300 MHz up to 10 GHz and the results are shown in figure 4. The breakdown voltage decreases with increasing frequency and shows a minimum at a pressure around 8 atm for the simulated conditions.

5. Conclusions

PIC simulations with MCCs have been performed to investigate the discharge breakdown mechanism in dc and RF discharges in micrometre and submicrometre size gaps. The dependence of the electron yield per ion on the electric field that incorporates ion-enhanced field emission has been used in the simulations. The incorporation of field emissions leads to deviations from the well-known Paschen curve in small gaps. The new Paschen curve obtained when the field emissions are accounted for, retains the right branch of

the conventional Paschen curve, i.e. field emissions can be neglected in large gaps. The left branch, however, is substituted by a rapid decrease of the breakdown voltage below the minimum of the conventional Paschen curve. This reduction in the breakdown voltage is observed for gap sizes smaller than 5 μm and is a direct consequence of the onset of field emissions. Good agreement is found between the simulation results and available experimental data.

The results of this paper should be useful for determining minimum ignition voltages in microplasma sources as well as the maximum safe operating voltage and critical dimensions in other microdevices.

Acknowledgments

This work was supported by the Lam Research Corporation and Tera-level Nano Devices Project, 21c Frontier R&D Program of Korea Ministry of Science and Technology.

References

[1] Franks A 1987 *J. Phys.* E **20** 1442
[2] Boyle W S, Kisliuk P and Germer L H 1955 *J. Appl. Phys.* **26** 720
[3] Germer L H 1959 *J. Appl. Phys.* **30** 46
[4] Fowler and Nordheim L 1928 *Proc. R. Soc. (London)* A **119** 173
[5] Korolev Yu D and Mesyats G A 1998 Physics of pulsed breakdown in gases (URO-PRESS)
[6] Bridsall C K 1991 *IEEE Trans. Plasm. Sci.* **19** 65
[7] Vahedi V and Surendra M 1995 *Comput. Phys. Commun.* **87** 179
[8] Petrovic Z Lj, Bzenic S, Jovanovic J and Djurovic S 1995 *J. Phys. D: Appl. Phys.* **28** 2287
[9] Surendra M and Graves D B 1990 *Appl. Phys. Lett.* **56** 1022
[10] Turner M M 1995 *Phys. Rev. Lett.* **75** 1312
[11] Lee J K and Verboncoeur J P 2001 Plasma display panel *Low Temperature Plasma Physics* ed R Hippler *et al* (New York: Wiley)
[12] Yang S S, Kim S J and Lee J K 2004 *J. Plasma Fusion Res.* **80** 132
[13] Wallash A and Honda M 1997 *EOS/ESD Symp. Proc. (EOS-19)* p 382
[14] Terashima K, Howald L, Haefke H and Guntherodt H-J 1996 *Thin Solid Films* **281–282** 634
[15] Germer L H 1958 *J. Appl. Phys.* **29** 1067
[16] Kisliuk P 1959 *J. Appl. Phys.* **30** 51
[17] Torres J M and Dhariwal R S 1999 *Nanotechnology* **10** 102
[18] Lee R T *et al* 2001 *Proc.-Sci. Meas. Technol.* **148** 8
[19] Slade P G and Taylor E D 2001 *IEEE Proc. Electron Control* 245
[20] Meek J M and Craggs J D 1953 *Electrical Breakdown of Gases* (Oxford: Oxford Unversity Press)
[21] Loeb L B 1939 *Fundamental Processes of Electrical Discharges in Gases* (New York: Wiley)
[22] Boyle W S and Kisliuk P 1955 *Phys. Rev.* **97** 255
[23] Germer L H and Haworth F E 1948 *Phys. Rev.* **73** 1121
[24] Newton R R 1948 *Phys. Rev.* **73** 1122
[25] Meek J M and Craggs J D 1978 *Electrical Breakdown in Gases* (New York: Wiley)
[26] Vaughan J R M 1989 *IEEE Trans.* **36** 1963
[27] Phelps A V and Petrović Z Lj 1999 *Plasma Sources Sci. Technol.* **8** R21
[28] Neyts E *et al* 2003 *J. Appl. Phys.* **93** 5025
[29] Verboncoeur J P *et al* 1993 *J. Comput. Phys.* **104** 321
[30] Lee J K *et al* 2004 *IEEE Trans. Plasma Sci.* **32** 47
[31] Kim H C and Lee J K 2004 *Phys. Rev. Lett.* **93** 085003
[32] Ito T, Izaki and Terashima K 2001 *Thin Solid Films* **386** 300
[33] Dhariwal R S, Torres J M and Desmulliez M P Y 2000 *IEE Proc.-Sci. Meas. Technol.* **147** 261
[34] Lee J K *et al AVS 51th Int. Sympo. & Exhibition (Anaheim, CA, 14–19 November 2004)* Invited Talk of Tech. Program, p 131